Unimolecular Isomerizations and Oxygen Atom Loss in Formaldehyde and Acetaldehyde Carbonyl Oxides. A Theoretical Investigation

Josep M. Anglada,*,† Josep M. Bofill,‡ Santiago Olivella,*,‡,§ and Albert Solé⊥

Contribution from the Centre d'Investigació i Desenvolupament del CSIC, Jordi Girona 18, 08034-Barcelona, Catalunya, Spain, and Departaments de Química Orgànica i Química Física, Universitat de Barcelona, Martí i Franquès 1, 08028-Barcelona, Catalunya, Spain

Received November 17, 1995. Revised Manuscript Received March 15, 1996[⊗]

Abstract: The lowest singlet and triplet potential energy surfaces of formaldehyde carbonyl oxide (**1**) and acetaldehyde carbonyl oxide (**2**) have been investigated in the regions concerning the most relevant unimolecular reactions by means of CASSCF and MRDCI ab initio quantum-chemical calculations. The questions related to the mechanism of O-atom loss from carbonyl oxides, as well as the competition between the cyclization to dioxirane and the tautomerization to hydroperoxide in methyl-substituted carbonyl oxides are addressed in this investigation. The theoretical predictions are consistent with experimental findings obtained from stopped-flow studies of the gas-phase ozonation of both *trans*-butene and tetramethylethylene. An unexpected result is that the most reasonable pathway for O-atom loss from "hot" singlet carbonyl oxides **1** and **2** involves internal rotation about the CO bond axis, followed by intersystem crossing to the lowest triplet state and subsequent scission of the OO bond.

I. Introduction

Formaldehyde carbonyl oxide (**1**) and acetaldehyde carbonyl oxide (**2**) are prototypical carbonyl oxides. Carbonyl oxides are established reactive intermediates in many oxidation reactions. Although carbonyl oxides were first postulated as intermediates in the ozonolysis of olefins by Criege in 1949,[1] direct experimental detection of a carbonyl oxide was not achieved until 1983 by means of time-resolved laser spectroscopy.[2] In the last few years, several groups have reported direct observations of carbonyl oxides.[3−7] The most important techniques for a direct spectroscopic characterization of carbonyl oxides have been matrix isolation[3,5] and laser photolysis.[2,6,7] The involvement of carbonyl oxides and their cyclic isomers, the dioxiranes (e.g., **1c** and **2c**), as short-lived reaction intermediates has been discussed in many oxidation reactions (e.g., ozonolysis, Baeyer−Villinger reaction)[8−10] and enzymatic processes.[11] Furthermore, carbonyl oxides are currently of interest because of their importance in the chemistry of urban air pollution,[12] and as chemical mimics of biological oxygen transfer systems.[13] The spectroscopic characterization, structure, and reactivity of carbonyl oxides has been the subject of recent reviews.[9,10b,14]

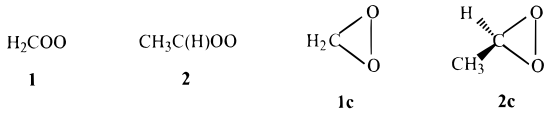

Carbonyl oxides are also interesting species from a theoretical point of view. Thus, quite a large number of theoretical studies of the electronic nature and structure of carbonyl oxides have been reported over the past 21 years.[15−26] High-level ab initio calculations have demonstrated that the inclusion of electron correlation effects into the quantum-chemical method employed

† Centre d'Investigació i Desenvolupament del CSIC.
‡ Departament de Química Orgànica, Universitat de Barcelona.
§ E-mail: olivella@taga.qo.ub.es.
⊥ Departament de Química Física, Universitat de Barcelona.
⊗ Abstract published in *Advance ACS Abstracts,* May 1, 1996.

(1) Criegee, R.; Wenner, G. *Chem. Ber.* **1949**, *564*, 9.
(2) Sugawara, T.; Iwamura, H.; Hayashi, H.; Sekiguchi, A.; Ando, W.; Liu, M. T. H. *Chem. Lett.* **1983**, 1261.
(3) (a) Bell, G. A.; Dunkin, I. R. *J. Chem. Soc., Chem. Commun.* **1983**, 1213. (b) Dunkin, I. R.; Bell, G. A. *Tetrahedron* **1985**, *41*, 339. (c) Bell, G. A.; Dunkin, I. R.; Shields, C. J. *Spectrochim. Acta* **1985**, *41A*, 1221. (d) Dunkin, I. R.; Shields, C. J. *J. Chem. Soc., Chem. Commun.* **1986**, *154*. (e) Dunkin, I. R.; Bell, G. A.; McCleod, F. G.; McCluskey, A. *Spectrochim. Acta* **1986**, *42A*, 567.
(4) (a) Sander, W. *Angew. Chem., Int. Ed. Engl.* **1986**, *25*, 255. (b) Sander, W. *Spectrochim. Acta* **1987**, *43A*, 637. (c) Sander, W. *J. Org. Chem.* **1988**, *53*, 125. (d) Sander, W. *J. Org. Chem.* **1988**, *53*, 2091. (e) Sander, W. *J. Org. Chem.* **1989**, *54*, 333.
(5) Ganzer, G. A.; Sheridan, R. S.; Liu, M. T. H. *J. Am. Chem. Soc.* **1986**, *108*, 1517.
(6) (a) Werstiuk, N. H.; Casal, H. L.; Scaiano, J. C. *Can. J. Chem.* **1984**, *62*, 2391. (b) Casal, H. L.; Tanner, M.; Werstiuk, N. H.; Scaiano, J. C. *J. Am. Chem. Soc.* **1985**, *107*, 4616. (c) Barcus, R. L.; Hadel, L. M.; Johnston, L. J.; Platz, M. S.; Savino, T. G.; Scaiano, J. C. *J. Am. Chem. Soc.* **1986**, *108*, 3928. (d) Scaiano, J. C.; McGimpsey, W. G.; Casal, H. L. *J. Org. Chem.* **1989**, *54*, 1612.
(7) (a) Fujiwara, Y.; Tanimoto, Y.; Itoh, M.; Hirai, K.; Tomioka, H. *J. Am. Chem. Soc.* **1987**, *109*, 1942. (b) Murata, S.; Tomioka, H.; Kawase, T.; Oda, M. *J. Org. Chem.* **1990**, *55*, 4502.
(8) Criegee, R. *Angew. Chem., Int. Ed. Engl.* **1975**, *14*, 745.
(9) Adam, W.; Curci, R.; Edwards, J. O. *Acc. Chem. Res.* **1989**, *22*, 205.
(10) (a) Murray, R. W.; Ramachandran, V. *Photochem. Photobiol.* **1979**, *30*, 187. (b) Murray, R. W. *Chem. Rev.* **1989**, *89*, 1187.
(11) Dix, T. A.; Benkovic, S. *Acc. Chem. Res.* **1988**, *21*, 101.
(12) (a) Atkinson, R.; Carter, W. P. L. *Chem. Rev.* **1984**, *84*, 437. (b) Atkinson, R.; Lloyd, A. *J. Phys. Chem. Ref. Data* **1984**, *13*, 315.
(13) Hamilton, G. A. In *Molecular Mechanisms of Oxygen Activation*; Hayashi, O., Ed.; Academic: New York, 1974; pp 245−283.
(14) (a) Kafafi, R. I.; Martinez, R. I., Herron, J. T. In *Molecular Structure and Energetics. Unconventional Chemical Bonding*; Liebman, J. F., Greenberg, A., Eds.; VCH Publishers: New York, 1988; Vol. 6, p 283. (b) Murray, R. W. In *Molecular Structure and Energetics. Unconventional Chemical Bonding*; Liebman, J. F., Greenberg, A., Eds.; VCH Publishers: New York, 1988; Vol. 6, p 311. (c) Sander, W. *Angew. Chem., Int. Ed. Engl.* **1990**, *29*, 344. (d) Bunnelle, W. *Chem. Rev.* **1991**, *91*, 335.
(15) Ha, T.-K.; Kühne, H.; Vaccani, S.; Günthard, H. H. *Chem. Phys. Lett.* **1974**, *24*, 172.
(16) (a) Wadt, W. R.; Goddard, W. A., III. *J. Am. Chem. Soc.* **1975**, *97*, 3004. (b) Harding, L. B.; Goddard, W. A., III. *J. Am. Chem. Soc.* **1978**, *100*, 7180.
(17) (a) Hiberty, P. *J. Am. Chem. Soc.* **1976**, *98*, 6088. (b) Hiberty, P.; Leforestier, C. *J. Am. Chem. Soc.* **1978**, *100*, 2012. (c) Hiberty, P. C.; Devidal, J. P. *Tetrahedron* **1979**, *68*, 4323.
(18) Hull, L. A. *J. Org. Chem.* **1978**, *43*, 2780.

S0002-7863(95)03858-3 CCC: $12.00

is essential for a reliable description of the electronic nature of carbonyl oxides.[20b,21g,i,26b] Because of the large computational effort involved, most of these high-level ab initio calculations have been restricted to the equilibrium structure of the electronic ground state (singlet) of the parent compound **1** and its cyclic isomer **1c**, as well as their interconversion. However, to our knowledge, no reliable ab initio calculations have been devoted yet to other potentially important unimolecular reactions of carbonyl oxides.

Recent experimental studies[27,28] aimed at understanding the mechanism of the photochemical smog production in polluted urban air have suggested that **1** and **2**, which are intermediates of the ozone reactions of ethylene, propylene, and 2-butene under atmospheric conditions, decay unimolecularly via numerous thermochemically accessible isomerization and dissociation channels. At present, mechanistic details of these unimolecular processes are not well established because of the lack of reliable kinetic data. Among the potentially important reaction channels suggested by early theoretical[10a] and experimental[29] studies is the unimolecular oxygen atom loss to produce the corresponding carbonyl compound (eq 1). There is some evidence that the

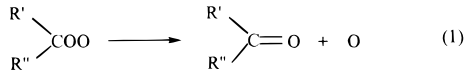

(1)

oxygen atoms are ejected in the O (^{3}P) electronic state.[30] This decomposition mode, designated the O-atom channel, competes with isomerization to the corresponding dioxirane (eq 2), which

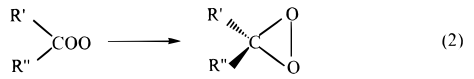

(2)

is sometimes the dominant reaction. For example, the gas-phase (1 atm) reaction of triplet methylene with O_2 leads to "hot" **1** (the reaction is estimated to be exothermic by 60 kcal/mol[14a]); among the decomposition products are ozone and formaldehyde.[31] These are formed by fragmentation of **1** to form formaldehyde plus an oxygen atom, which recombines with O_2 to provide ozone. In this system, the O-atom channel amounts to an estimated[14a] 1−5% of the total **1** consumption. A substantial energy barrier is indicated by the fact that **1** produced in the less-energetic ethylene ozonolysis does not produce oxygen atoms at a detectable level.[32]

For carbonyl oxides with α-hydrogens, tautomerization to the corresponding hydroperoxide (eq 3) involving a 1,4 H-atom

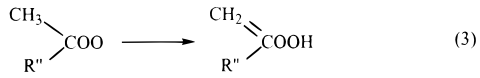

(3)

migration from carbon to oxygen appears to be a competitive isomerization pathway. For instance, kinetic modeling of the results obtained in stopped-flow studies of gas-phase ozonation of *trans*-butene suggests that at least 10% of the total carbonyl oxide **2** formed decomposes via this hydroperoxide channel, while the O-atom channel contributes on the order of ≤5% to its decomposition.[28b] In this system, kinetic modeling also leads to an estimate that at least 10% of **2** follows the isomerization to **2c** pathway. In clear contrast, similar kinetic modeling studies on the mechanisms of gas-phase ozonolysis of tetramethylethylene indicate that 80% of the acetone carbonyl oxide (**3**) formed follows tautomerization to the corresponding hydroperoxide, while isomerization to dimethyldioxirane (**3c**) is negligible.[28a]

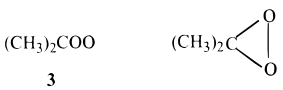

3 **3c**

Another issue of considerable interest in connection with potential unimolecular isomerization reactions of methyl-substituted carbonyl oxides is the *syn/anti* interconversion. For instance, two stereoisomers *syn* and *anti* (**2d** and **2e**, respectively) are possible for carbonyl oxide **2**. Ab initio calculations

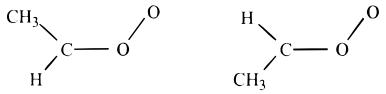

2d **2e**

accounting for electron correlation through second-order Møller−Plesset perturbation theory (MP2) indicate that **2d** is 3.3 kcal/mol more stable than **2e** and that they are separated by an interconversional energy barrier of 35.6 kcal/mol.[21a] Therefore, it is reasonable to expect configurational stability of the *syn* and *anti* stereoisomers, which then might display different reactivities.

For the purposes of atmospheric modeling, it is of considerable interest to know the energy barriers and the energies of reaction for the above unimolecular processes. In this spirit we have investigated the CH_2O_2 and $C_2H_4O_2$ singlet and triplet potential energy surfaces (PESs) in the regions concerning the most relevant unimolecular reactions of **1** and **2** by means of high-level ab initio quantum-chemical calculations. In particular we address the questions related to the mechanism of oxygen atom loss from carbonyl oxides, as well as the competition between the cyclization to dioxirane and the tautomerization to hydroperoxide in methyl-substituted carbonyl oxides. We present here the results of this theoretical investigation. Furthermore, we also report in this paper the harmonic vibrational frequencies and infrared (IR) intensities calculated for the equilibrium structures on the aforementioned PESs, as well as the vertical electronic excitation energies calculated for the

(19) (a) Yamaguchi, K.; Ohta, K.; Yabushita, S.; Fueno, T. J. *J. Chem. Phys.* **1978**, *68*, 4323. (b) Yamaguchi, K.; Yabushita, S.; Fueno, T. J.; Morokuma, K.; Iwata, S. *Chem. Phys. Lett.* **1980**, *71*, 563. (c) Yamaguchi, K. *J. Mol. Struct.*: *THEOCHEM* **1983**, *103*, 101.

(20) (a) Karlström, G.; Engström, S.; Jönsson, B. *Chem. Phys. Lett.* **1979**, *67*, 343. (b) Karlström, G.; Roos, B. O. *Chem. Phys. Lett.* **1981**, *79*, 416.

(21) (a) Cremer, D. *J. Am. Chem. Soc.* **1979**, *101*, 7199. (b) Cremer, D. *J. Am. Chem. Soc.* **1981**, *103*, 3619, 3627, 3633. (c) Cremer, D. *Angew. Chem., Int. Ed. Engl.* **1981**, *20*, 888. (d) Cremer, D. In *The Chemistry of Functional Groups, Peroxides*; Patai, S., Ed.; Wiley: New York, 1983; p 1. (e) Gauss, J.; Cremer, D. *Chem. Phys. Lett.* **1987**, *133*, 420. (f) Cremer, D.; Schmidt, T.; Gauss, J.; Radhakrisnan, T. P. *Angew. Chem., Int. Ed. Engl.* **1988**, *27*, 427. (g) Gauss, J.; Cremer, D. *Chem. Phys. Lett.* **1989**, *163*, 549. (h) Cremer, D.; Schmidt, T.; Sander, W.; Bischof, P. *J. Org. Chem.* **1989**, *54*, 2515. (i) Cremer, D.; Gauss, J.; Kraka, E.; Stanton, J. F.; Bartlett, R. *J. Chem. Phys. Lett.* **1993**, *209*, 547.

(22) Kahn, S. D.; Hehre, W. J.; Pople, J. A. *J. Am. Chem. Soc.* **1987**, *109*, 1871.

(23) Rahman, M.; McKee, M.; Shevlin, P. B.; Sztybicka, R. *J. Am. Chem. Soc.* **1988**, *110*, 4002.

(24) Steinke, T.; Hänsele, E.; Clark, T. *J. Am. Chem. Soc.* **1989**, *111*, 9107.

(25) Yang, C.; You-Liang, W. *J. Mol. Struct.: THEOCHEM* **1990**, *204*, 285.

(26) (a) Bach, R. D.; Owensby, A. L.; Andrés, J. L.; Schlegel, H. B. *J. Am. Chem. Soc.* **1991**, *113*, 7031. (b) Bach, R. D.; Andrés, J. L.; Owensby, A. L.; Schlegel, H. B.; McDouall, J. J. W. *J. Am. Chem. Soc.* **1992**, *114*, 7207.

(27) Niki, H.; Maker, P. D.; Savage, C. M.; Breitenbach, L. P.; Hurley, M. D. *J. Phys. Chem.* **1987**, *91*, 941.

(28) (a) Martinez, R. I.; Herron, J. T. *J. Phys. Chem.* **1987**, *91*, 946. (b) Martinez, R. I.; Herron, J. T. *J. Phys. Chem.* **1988**, *92*, 4644.

(29) Martinez, R. I.; Herron, J. T.; Huie, R. E. *J. Am. Chem. Soc.* **1981**, *103*, 3807.

(30) Sander, W. *Angew. Chem., Int. Ed. Engl.* **1985**, *24*, 988.

(31) Hatakeyama, S.; Bandow, H.; Okuda, M.; Akimoto, H. *J. Phys. Chem.* **1981**, *85*, 2249.

(32) Niki, H.; Maker, P. D.; Savage, C. M.; Breitenbach, L. P.; Martinez, R. I. *J. Phys. Chem.* **1984**, *88*, 766.

singlet ground state of **1** and **2**. It is hoped that these spectroscopic data will prove to be helpful in aiding the identification of **1**, **2**, or their isomerization products in future matrix-isolation and time-resolved laser spectroscopy experiments.

II. Methods and Computational Details

Two basis sets have been used in this study. The basis set designated A is the split-valence d-polarized 6-31G* basis.[33] The other basis set, designated B, is the standard Huzinaga−Dunning double-ζ basis ((9s5p/4s2p) contractions for C and O, (4s/2s) for H),[34,35] augmented by a diffuse p-type function on C and O (orbital exponents $\alpha_p(C) = 0.034$[36] and $\alpha_p(O) = 0.05$[37]), two d-type polarization functions on C and O (orbital exponents $\alpha_d(C) = 1.097$ and 0.318 and $\alpha_d(O) = 2.314$ and 0.645[38]), and a p-type polarization function on H (orbital exponent $\alpha_p(H) = 1.0$[39]).

The molecular geometries of the stationary points located on the aforementioned PESs were optimized by use of multiconfiguration SCF (MCSCF) wave functions of the complete active space (CAS) SCF class[40] employing analytical gradient procedures.[41,42] The CASs were selected following the procedure recently suggested by Anglada and Bofill,[43] based on the fractional occupation of the natural orbitals (NOs) generated from the first-order density matrix calculated from an initial multireference single- and double-excitation configuration interaction (MRDCI) wave function correlating all valence electrons. Thus, for the singlet state of **1** (C_s molecular symmetry) the fractional occupancies of the NOs indicated that there are eight *active* orbitals. These are four molecular orbitals (MOs) of a′ symmetry, which correspond to the bonding and antibonding orbitals of the CO and OO σ bonds, and four MOs of a″ symmetry. The latter MOs are the three π orbitals formally generated within the framework of a minimum basis set, and one (CO bonding) of the additional three π orbitals arising from the utilization of a split-valence basis set. Distribution of the corresponding eight *active* electrons, namely, four σ electrons and four π electrons, among these eight *active* orbitals leads to CASSCF(8,8) wave functions formed as a linear combination of 1764 and 2352 spin-adapted configuration state functions (CSFs) for the singlet and triplet states, respectively, in C_1 symmetry. For the singlet state of **1c** (C_{2v} molecular symmetry), the aforementioned active space selection procedure led to a CAS formed by three MOs of a_1 symmetry (the linear combinations of the bonding orbitals of the two CO and the OO σ bonds), three MOs of b_2 symmetry (the linear combinations of the antibonding orbitals of the two CO and the OO σ bonds), and three π MOs (two of b_1 symmetry and one of a_2 symmetry). Distribution of the corresponding ten *active* electrons, namely, six σ electrons and four π electrons, among these nine *active* orbitals leads to CASSCF(10,9) wave functions formed as a linear combination of 5292 CSFs in C_1 symmetry. Regarding the other stationary points located on the PESs, the active space selection procedure used led to a CASSCF(8,8) wave function similar to that employed in the geometry optimization of both the singlet and triplet states of **1**.

The normal modes and harmonic vibrational frequencies of the equilibrium and transition structures optimized at the CASSCF level of theory were obtained by diagonalizing the mass-weighted Cartesian force constant matrix calculated numerically by finite differences of analytical gradients.[44a] The dipole moment derivatives which determine the IR intensities were determined by numerically differentiating the dipole moments with respect to the nuclear coordinates and transforming them to normal coordinates.[44b] The zero-point vibrational energies (ZPVEs) were determined from the harmonic vibrational frequencies scaled by 0.8929 (the reciprocal of 1.12).[45] The A basis set was used for the CASSCF calculations of all the stationary points on the singlet and triplet PESs of both **1** and **2**. To establish that our results are converged with respect to the basis set, additional CASSCF calculations with the B basis set were performed for the stationary points concerning the isomerization of singlet **1** to **1c**. All CASSCF calculations were carried out by using the GAMESS system of programs.[46]

To incorporate the effect of dynamical valence-electron correlation on the relative energy ordering of the calculated stationary points, as well as the vertical electronic transition energies, MRDCI calculations were carried out at the CASSCF optimum geometries using the program package of Buenker and Peyerimhoff,[47] which includes a table CI algorithm and extrapolation techniques. In this MRDCI treatment the reference set consists of all configurations which appear in the final CI expansion with a coefficient of roughly $c^2 \geq 0.02$. The SCF MOs for the respective states are employed to construct the configurations; all nonvalence MOs are frozen. Configuration selection is undertaken at a threshold T in a standard manner,[47a] and the resulting secular equation is solved directly. Next, the first-order density matrix corresponding to this MRDCI calculation employing SCF MOs is simply diagonalized for obtaining the NOs, which are subsequently employed in a final MRDCI calculation. The effect of the remaining configurations of the total MRDCI space on the energy of the system is accounted for by a self-correcting perturbation-type (extrapolation) procedure.[47b,c] Finally, the energy corresponding to the full CI space of the given basis set, designated E(MRDCI+Q), is estimated in analogy to the formula given by Langhoff and Davidson[48] as

$$E(\text{MRDCI+Q}) = E(\text{MRDCI}) + (1 - \sum c_0^2)(E(\text{MRDCI}) - E(\text{ref})) \quad (4)$$

where the sum is taken over all CSFs in the reference set, and E(MRDCI) and E(ref) are the total energies of the MRDCI and reference set wave functions.[49]

The MRDCI calculations of the stationary points on the CH_2O_2 singlet and triplet PESs were carried out with both the A ($T = 2$ μhartrees) and B ($T = 3$ μhartrees) basis sets, while those of the $C_2H_4O_2$ singlet and triplet PESs were carried out only with the A basis ($T = 4$ μhartrees). The size of the generated MRDCI spaces varied roughly from 6×10^5 to 22×10^6, while the size of the selected subspaces, namely, the dimensions of the secular equations actually solved, was on the order of 17000−32000.

III. Results

A. Nomenclature. The calculated structures are named as follows. The structures of the stationary points on the CH_2O_2 singlet and triplet PESs are designated by **SA** and **TA**, respectively, while those on the $C_2H_4O_2$ singlet and triplet PESs are designated by **SB** and **TB**, respectively. The label of the structures corresponding to transition states are followed by the letters **TS**. The structures are distinguished from each other

(33) Hariharan, P. C.; Pople, J. A. *Theor. Chim. Acta* **1973**, *28*, 213.
(34) Huzinaga, S. *J. Chem. Phys.* **1965**, *42*, 1293.
(35) Dunnig, T. H. *J. Chem. Phys.* **1970**, *53*, 2823.
(36) Dunnig, T. H.; Hay, P. J. In *Modern Theoretical Chemistry*; Schaefer, H. F., Ed.; Plenum: New York, 1977; Vol. 3, p 1.
(37) Banichevich, A.; Peyerimhoff, S. D. *Chem. Phys.* **1993**, *174*, 93.
(38) Dunning, T. H. *J. Chem. Phys.* **1989**, *90*, 1007.
(39) Bauschlicher, C. W., Jr. *J. Chem. Phys.* **1986**, *85*, 6510.
(40) For a review, see: Roos, B. O. *Adv. Chem. Phys.* **1987**, *69*, 399.
(41) (a) Baker, J. *J. Comput. Chem.* **1986**, *7*, 385. (b) Baker, J. *J. Comput. Chem.* **1987**, *8*, 563.
(42) Bofill, J. M. *J. Comput. Chem.* **1994**, *15*, 1.
(43) Anglada, J. M.; Bofill, J. M. *Chem. Phys. Lett.* **1995**, *243*, 151.
(44) (a) Pulay, P. In *Modern Theoretical Chemistry*; Schaefer, H. F., Ed.; Plenum: New York, 1977; Vol. 4, p 153. (b) Pulay, P.; Fogarasi, G.; Pang, F.; Boggs, J. E. *J. Am. Chem. Soc.* **1979**, *101*, 2550.
(45) Curtiss, L. A.; Raghavachari, K.; Trucks, G. W.; Pople, J. A. *J. Chem. Phys.* **1991**, *94*, 7221.
(46) Schmidt, M. W.; Baldrige, K. K.; Boatz, J. A.; Jensen, J. H.; Koseki, S.; Gordon, M. S.; Nguyen, K. A.; Windus, T. L.; Elbert, S. T. Gamess. *QCPE Bull.* **1990**, *10*, 52.
(47) (a) Buenker, R. J.; Peyerimhoff, S. D. *Theor. Chim. Acta* **1974**, *35*, 33. (b) Buenker, R. J.; Peyerimhoff, S. D. *Theor. Chim. Acta* **1975**, *39*, 217. (c) Buenker, R. J.; Peyerimhoff, S. D.; Butscher, W. *Mol. Phys.* **1978**, *35*, 771. (d) Buenker, R. J.; Peyerimhoff, S. D. In *New Horizons of Quantum Chemistry*; Lowdin, P. O., Pullman, B., Eds.; D. Reidel: Dordrecht, The Netherlands, 1983; p 183. (e) Buenker, R. J.; Philips, R. A. *J. Mol. Struct.*: *THEOCHEM* **1985**, *123*, 291.
(48) Davidson, E. R. In *New Horizons of Quantum Chemistry*: Lowdin, P. O., Pullman, B., Eds.; D. Reidel: Dordrecht, The Netherlands, 1983; p 17. (b) Langhoff, S. R.; Davidson, E. R. *Int. J. Quantum Chem.* **1974**, *8*, 61.
(49) (a) Buenker, R. J.; Peyerimhoff, S. D.; Bruna, P. J. In *Computational Theoretical Organic Chemistry*; Csizmadia, I. G.; Daudel, R., Eds.; D. Reidel: Dordrecht, The Netherlands, 1981; p 55. (b) Burton, P. G.; Buenker, R. J.; Bruna, P. J.; Peyerimhoff, S. D. *Chem. Phys. Lett.* **1983**, *95*, 379.

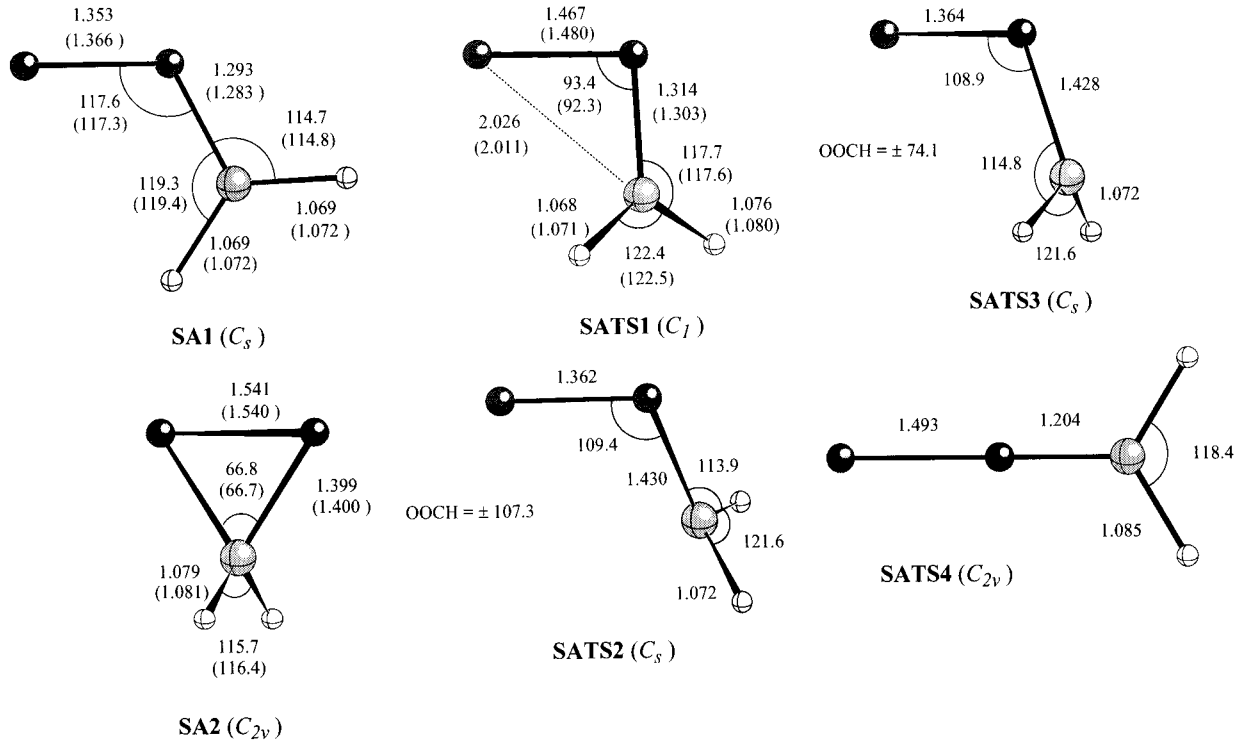

Figure 1. Selected geometrical parameters of the CASSCF/basis A optimized structures for the stationary points located on the CH_2O_2 singlet ground-state potential energy surface. Distances are given in angstroms and angles in degrees. The values calculated with the B basis set are given in parentheses.

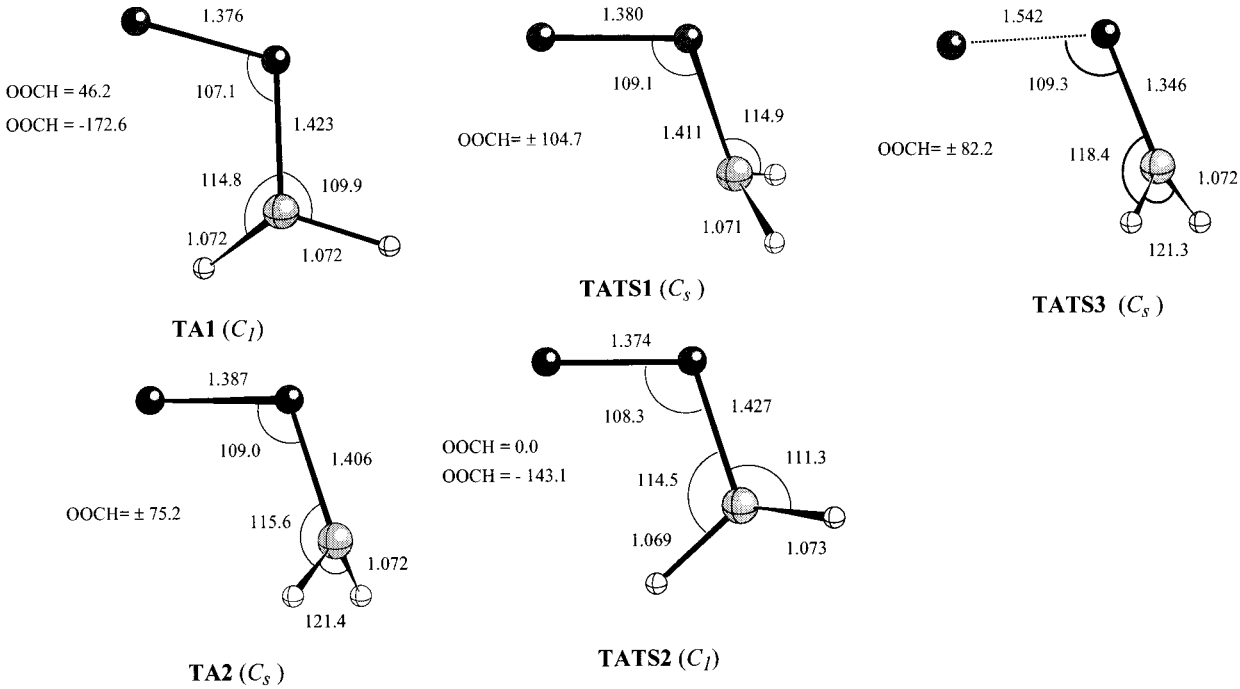

Figure 2. Selected geometrical parameters of the CASSCF/basis A optimized structures for the stationary points located on the CH_2O_2 lowest triplet state potential energy surface. Distances are given in angstroms and angles in degrees.

by appending the numbers **1**, **2**, etc., as they are introduced. For example, structure **SA2** is the second equilibrium structure on the CH_2O_2 singlet PES, while structure **TBTS3** is the third transition structure on the $C_2H_4O_2$ triplet PES.

B. Molecular Geometries. The Cartesian coordinates of all structures reported in this paper are available as supporting information. The most relevant geometrical parameters of the CASSCF/basis A optimized structures for the stationary points located on the CH_2O_2 singlet and triplet PESs are given in Figures 1 and 2, respectively. For comparison, the geometrical parameters obtained with the B basis set for structures **SA1**, **SA2**, and **SATS1** are shown in parentheses. The most relevant geometrical parameters of the CASSCF/basis A optimized structures of the stationary points located on the $C_2H_4O_2$ singlet and triplet PESs are given in Figures 3 and 4, respectively.

C. Energies, Dipole Moments, and Dissociation Energies. The total energies, ZPVEs, and dipole moments calculated at the CASSCF level of theory with the A basis set for the stationary points located on the CH_2O_2 singlet and triplet PESs are collected in Table 1 of the supporting information, together with the total energies calculated at the MRDCI and MRDCI+Q levels with the A and B basis sets. The MRDCI and MRDCI+Q relative energies are given in Table 1. The last column of Table 1 also gives the relative energies calculated at

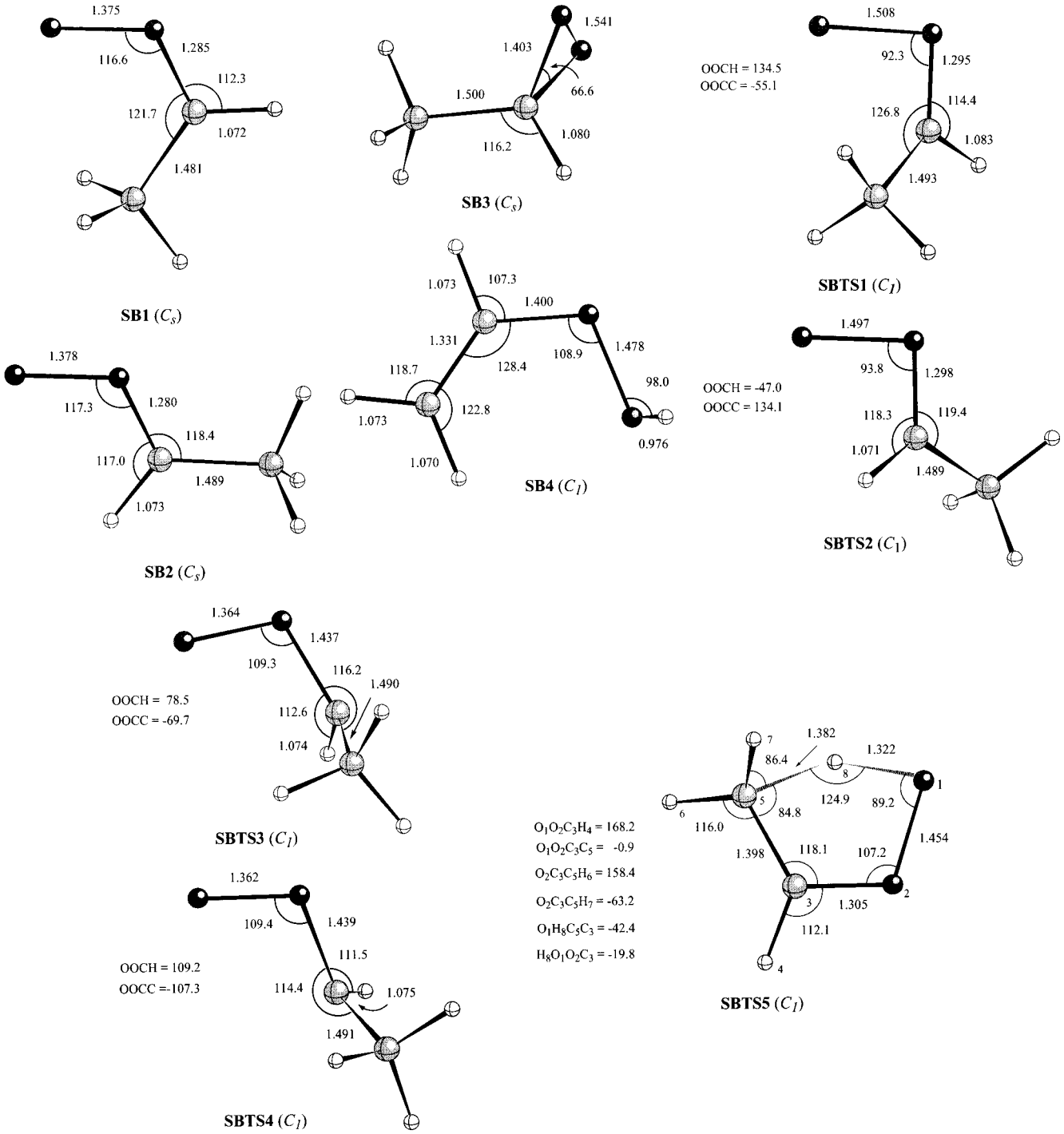

Figure 3. Selected geometrical parameters of the CASSCF/basis A optimized structures for the stationary points located on the $C_2H_4O_2$ singlet ground-state potential energy surface. Distances are given in angstroms and angles in degrees.

the MRDCI+Q level with the B basis set including the ZPVE correction. All calculations were performed using the CASSCF/basis A optimized geometries.

The CASSCF/basis A total energies, ZPVEs, and dipole moments of the stationary points located on the $C_2H_4O_2$ singlet and triplet PESs are collected in Table 2 of the supporting information, along with the total energies calculated at the MRDCI and MRDCI+Q levels of theory with the A basis set. The MRDCI and MRDCI+Q relative energies are given in Table 2. The last column of Table 2 also gives the relative energies calculated at the MRDCI+Q level including the ZPVE correction. Figures 5 and 6 provide schematic potential energy diagrams for the stationary points on the singlet and triplet PESs, respectively, based on the relative energies calculated at the latter level of theory.

Finally, the MRDCI+Q dissociation energies of the lowest singlet and triplet states of **1** and **2** for oxygen atom loss, either in its ground (^{3}P) or lowest singlet (^{1}D) state, are given in Table 3. The ZPVE corrected values are given in parentheses.

Unless otherwise noted, the relative energies and the dissociation energies of the stationary points on the CH_2O_2 singlet and triplet PESs given hereafter in the text refer to the MRDCI+Q/basis B plus ZPVE correction values, while those of the stationary points on the $C_2H_4O_2$ singlet and triplet PESs refer to the MRDCI+Q/basis A plus ZPVE correction values.

D. Vibrational Frequencies. The harmonic vibrational frequencies calculated for the equilibrium structures of the CH_2O_2 singlet (**SA1** and **SA2**) and triplet (**TA1** and **TA2**) and $C_2H_4O_2$ singlet (**SB1**, **SB2**, **SB3**, and **SB4**) and triplet (**TB1**, **TB2**, and **TB3**) PESs are given in Tables 3−10 of the supporting

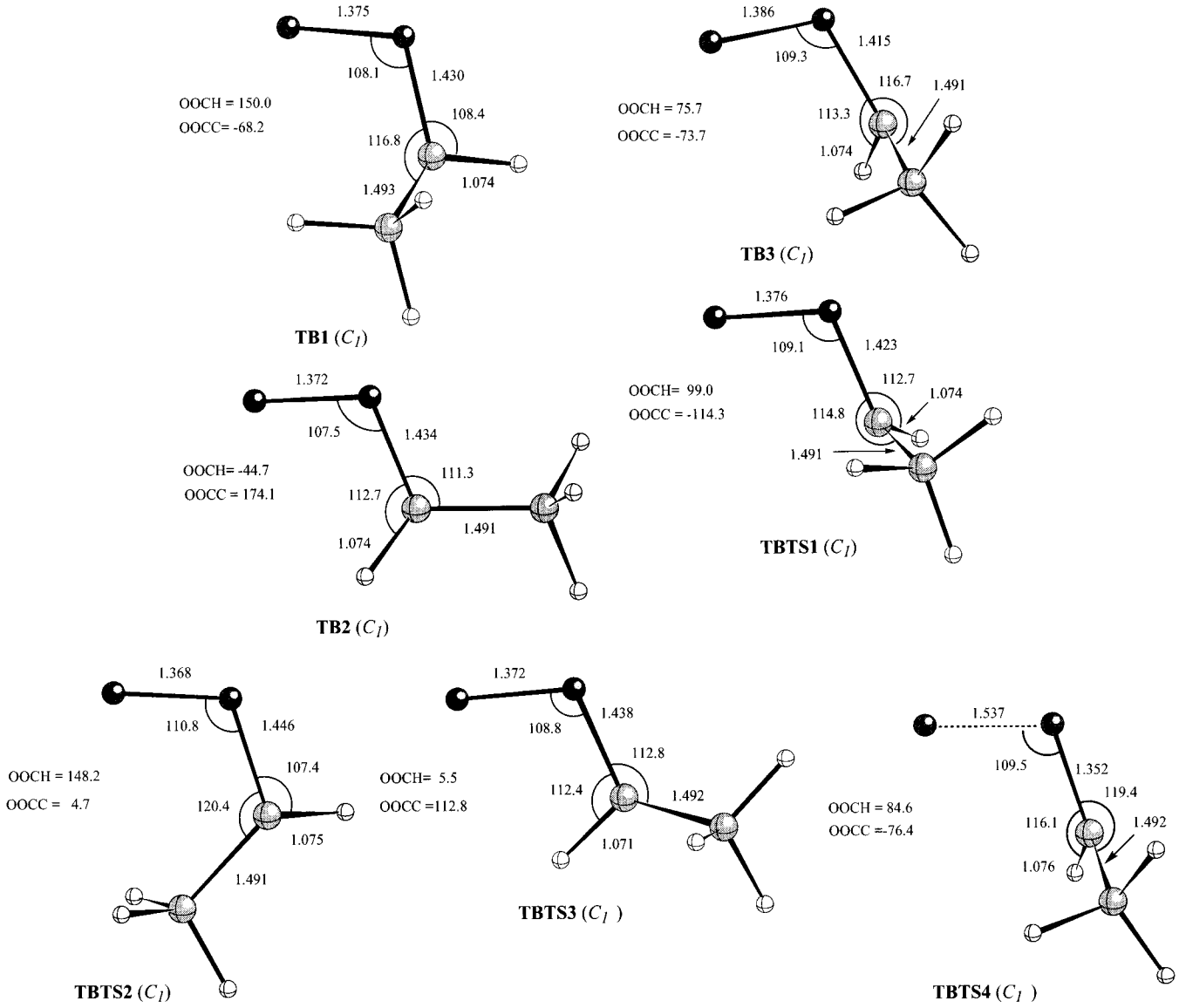

Figure 4. Selected geometrical parameters of the CASSCF/basis A optimized structures for the stationary points located on the $C_2H_4O_2$ lowest triplet state potential energy surface. Distances are given in angstroms and angles in degrees.

Table 1. Relative Energies (kcal/mol) for CASSCF/basis A Optimized Structures of the Stationary Points on the Singlet and Triplet CH_2O_2 Potential Energy Surfaces

structure	MRDCI/basis A	MRDCI+Q/basis A	MRDCI/basis B	MRDCI+Q/basis B	MRDCI+Q/basis B + ZPVE
			Singlet Potential Energy Surface		
SA1	0.0	0.0	0.0	0.0	0.0
SA2	−33.5	−31.1	−30.2	−29.9	−28.5
SATS1	25.9	25.8	26.2	24.9	24.0
SATS2	27.8	29.0	29.0	27.5	26.0
SATS3	27.9	28.8	28.6	27.1	25.7
SATS4	37.6	40.5	38.5	37.8	
			Triplet Potential Energy Surface		
TA1	2.3	1.9	4.4	5.6	5.7
TA2	0.0	0.0	0.0	0.0	0.0
TATS1	3.2	1.8	3.6	1.8	1.4
TATS	4.4	2.9	4.0	2.2	2.3
TATS3	5.7	3.9	5.3	4.7	3.7

information. Along with the frequencies, the symmetry, approximate description, and IR intensity of each normal mode are indicated in these tables.

E. Vertical Electronic Excitation Energies. The MRDCI+Q vertical excitation energies calculated for the singlet ground state of **1** and the *syn* and *anti* stereoisomers of **2** are given in Table 11 of the supporting information. Approximate descriptions of the main electronic transition leading to the excited state associated with each vertical excitation are also given in this table.

IV. Discussion

A. Formaldehyde Carbonyl Oxide. 1. Singlet and Triplet Equilibrium Structures. Overall, the geometrical

Table 2. Relative Energies (kcal/mol) for CASSCF/basis A Optimized Structures of the Stationary Points on the Singlet and Triplet $C_2H_4O_2$ Potential Energy Surfaces

structure	MRDCI/basis A	MRDCI+Q/basis A	MRDCI+Q/basis A + ZPVE
		Singlet Potential Energy Surface	
SB1	0.0	0.0	0.0
SB2	3.7	2.5	2.2
SB3	−29.4	−29.1	−28.2
SBTS1	30.8	29.2	28.4
SBTS2	25.8	23.9	22.8
SBTS3	35.9	34.3	33.0
SBTS4	34.1	31.9	30.5
SBTS5	25.4	22.0	21.2
SB4	−17.2	−19.4	−20.2
		Triplet Potential Energy Surface	
TB1	0.0	0.0	0.0
TB2	1.8	3.0	3.0
TB3	−1.5	0.0	0.0
TBTS1	3.3	3.8	3.3
TBTS2	6.5	7.2	7.1
TBTS3	4.2	3.5	3.3
TBTS4	1.7	1.9	0.5

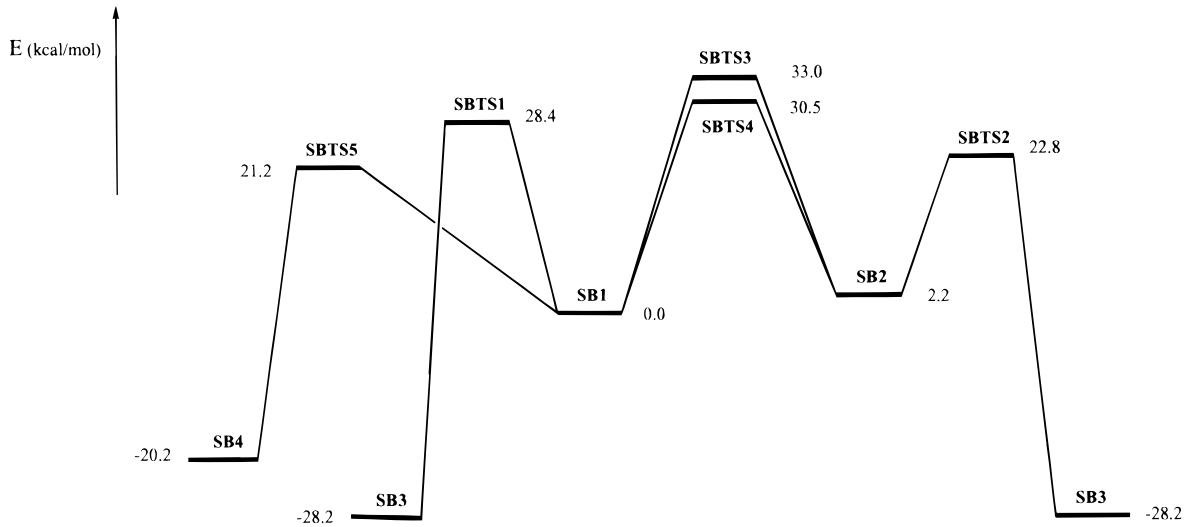

Figure 5. Schematic potential energy diagram showing the relative energies of the stationary points located on the $C_2H_4O_2$ singlet ground-state potential energy surface. Energy values were obtained from the ZPVE-corrected MRDCI+Q/basis A energies relative to that of **SB1**.

parameters calculated for the singlet ground state of **1** (**SA1**) and **1c** (**SA2**) using the A basis set are similar to those calculated with the larger B basis set. Thus, the bond distance differs by up to 0.013 Å (OO bond of **SA1**), while the bond angle differs by up to 0.7° (HCH angle of **SA2**). Unless otherwise noted, the geometries discussed in the following sections refer to the geometries calculated with the A basis set. As mentioned in the Introduction, the calculated equilibrium structure of singlet **1** is particularly sensitive to the method used to account for the electron correlation. Therefore, it is gratifying that the predicted relevant geometrical parameters of **SA1** are in good agreement with the values (i.e., R(OO) = 1.355 Å, R(CO) = 1.290 Å, $\angle$(COO) = 117.8°, $\angle(OCH_{syn}) = 118.7°$, $\angle(OCH_{anti}) = 115.1°$) obtained from coupled cluster (CC) calculations including all single and double excitations together with a perturbative estimation of the triple excitations (CCSD(T)) employing the A basis set.[43] As pointed out by Cremer *et al.*[21i] CCSD(T) theory has proven to yield reliable results in cases where the correlation energy plays a crucial role in determining the molecular geometry.[50] Hence, our CASSCF calculations appear to provide a suitable description of **1**. An interesting aspect of the equilibrium structure predicted for **1** is that the CO and OO distances of **SA1** suggest a significant double bond character of these bonds. This reveals that the electronic structure of singlet **1** possesses more zwitterionic character than expected in the grounds of previous generalized valence bond (GVB) and MP2 calculations.

Regarding **1c**, the reliability of our calculations can be assessed by comparing the relevant geometrical parameters of **SA2** with the reported experimental data obtained from microwave spectroscopy (i.e., R(OO) = 1.516 Å, R(CO) = 1.388 Å, $\angle$(COO) = 66.2°, $\angle$(HCH) = 117.3°).[51] Except the OO bond distance, which is 0.025 Å too long, the calculated geometrical parameters are in good agreement with these data. Furthermore, the calculated dipole moment of 2.71 D is reasonably close to the experimental value of 2.48 D.[51]

The most remarkable geometrical feature of the lowest triplet state of **1** is the strong pyramidalization at the carbon atom. Earlier ab initio calculations[16,21a,25] have assumed for this state a twisted C_s structure in which the plane of the carbon atom (sp^2 hybridization) has been rotated 90° with respect to the

(50) (a) Rendell, A. P.; Lee, T. L.; Taylor, P. R. *J. Chem. Phys.* **1990**, *92*, 7050. (b) Lee, T. L.; Scuseria, G. E. *J. Chem. Phys.* **1990**, *93*, 489. (c) Scuseria, G. E.; Lee, T. L. *J. Chem. Phys.* **1990**, *93*, 5851. (d) Watts, J. D.; Cernusak, I.; Noga, J.; Bartlett, R. J.; Bauschlicher, C. W.; Lee, T. J.; Rendell, A.; Taylor, P. R. *J. Chem. Phys.* **1990**, *93*, 8875. (e) Watts, J. D.; Stanton, J. F.; Bartlett, R. J. *Chem. Phys. Lett.* **1991**, *178*, 471. (f) Bentley, J. A.; Bowman, J. M.; Gadzy, B.; Lee, T. L.; Dateo, C. E. *Chem. Phys. Lett.* **1992**, *198*, 563. (g) Watts, J. D.; Gauss, J.; Stanton, J. F.; Bartlett, R. J. *J. Chem. Phys.* **1992**, *97*, 8372.

(51) (a) Lovas, F. J.; Suenram, R. D. *Chem. Phys. Lett.* **1977**, *51*, 453. (b) Suenram, R. D.; Lovas, F. J. *J. Am. Chem. Soc.* **1978**, *100*, 5117.

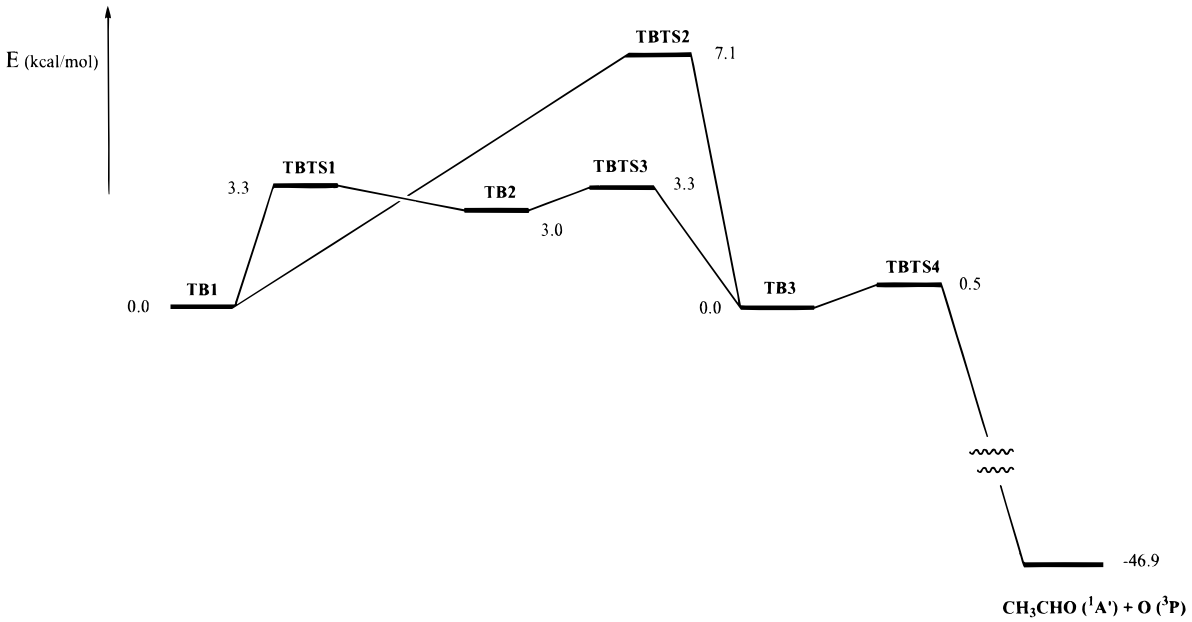

Figure 6. Schematic potential energy diagram showing the relative energies of the stationary points located on the $C_2H_4O_2$ lowest triplet state potential energy surface. Energy values were obtained from the ZPVE-corrected MRDCI+Q/basis A energies relative to that of **TB1**.

Table 3. MRDCI+Q Dissociation Energies (kca/mol) of the Lowest Singlet and Triplet States of Formaldehyde and Acetaldehyde Carbonyl Oxides for Oxygen Atom Loss[a,b]

dissociation channel	basis set A	basis set B
$H_2COO(^1A')\rightarrow H_2CO(^1A_1) + O(^1D)$	37.7 (35.5)	34.6 (32.4)
$H_2COO(^3A'')\rightarrow H_2CO(^1A_1) + O(^3P)$	−38.9 (−39.7)	−40.0 (−40.8)
$CH_3(H)COO(syn)(^1A')\rightarrow CH_3(H)CO(^1A) + O(^1D)$	34.1 (32.0)	
$CH_3(H)COO(anti)(^1A')\rightarrow CH_3(H)CO(^1A) + O(^1D)$	31.6 (29.8)	
$CH_3(H)COO(^3A)\rightarrow CH_3(H)CO(^1A) + O(^3P)$	−45.7 (−46.9)	

[a] MRDCI+Q energies of the dissociation products (hartrees): −114.18800 (H_2CO ($^1A_1$), basis A), −114.25783 (H_2CO ($^1A_1$), basis B), −153.36549 ($CH_3(H)CO$ (^1A)), −74.89773 (O (^3P), basis A), −74.93865 (O (^3P), basis B), −74.81809 (O (^1D), basis A), and −74.86038 (O (^1D), basis B). [b] ZPVE corrected values are given in parentheses.

planar equilibrium geometry of the singlet ground state, making the HCH plane perpendicular to the COO plane. For an OO bond distance ranging from 1.374 to 1.387 Å and a CO bond distance ranging from 1.406 to 1.427 Å, we have found four stationary points on the PES of the lowest triplet state. The corresponding optimized structures, namely, **TA1**, **TA2**, **TATS1**, and **TATS2**, differentiate in the OOCH dihedral angles, which determine the rotation angle between the HCH and COO planes and the pyramidalization at the carbon atom. **TA1** and **TA2** are true local minima on the CASSCF PES, while **TATS1** and **TATS2** correspond to rotational transition states connecting these minima. However, at the highest level of theory employed in this study, namely, MRDCI+Q/basis B with ZPVE correction, the local minimum **TA1** lies higher in energy than the transition structures **TATS1** and **TATS2**. Therefore, it appears that **TA2** is the lowest energy equilibrium structure of triplet **1**. A comparison of the structures calculated for the lowest singlet and triplet states of **1** (i.e., **SA1** and **TA2**) reveals that in passing from **SA1** to **TA2** the CO bond distance lengthens from 1.293 to 1.406 Å, while the OO bond distance is lengthened only by 0.034 Å. These geometrical changes indicate that the two unpaired electrons of the lowest triplet state essentially correspond to the electrons forming the CO π bond in the singlet ground state. The dominant electronic configuration of the MRDCI wave function of this triplet state can be written as ... $10a'^1\ 3a''^1$, so it turns out to be of A″ symmetry. Finally, it is worthy mentioning that the 10a′ MO is localized on the carbon atom, while the 3a″ MO is mainly localized on the terminal oxygen atom.

2. Cyclization to Dioxirane. As noted in earlier theoretical studies,[20b,21f,i,26] the geometry of the transition structure (**SATS1**) calculated for the isomerization of singlet ground-state **1** to **1c** more closely resembles **SA1** than **SA2**, with the exception of the OO bond distance (1.467 Å) which is 0.114 Å longer at the transition structure. This is also suggested by the long CO distance of 2.026 Å, which is closer to that (2.281 Å) in **SA1** than that (1.399 Å) in **SA2**. Furthermore, despite the rotation of the CH_2 group with respect to the OOC plane in **SATS1** (47.4°), the pyramidalization at the carbon atom is negligible. The **1** → **1c** isomerization is calculated to be exothermic by 28.5 kcal/mol with an energy barrier of 24.0 kcal/mol. These values are somewhat high as compared with the exothermicity of 24.2 kcal/mol and the energy barrier of 20.3 kcal/mol predicted at the CCSD(T)/DZ+P level of theory.[21i] The calculated energy barrier should be sufficiently small that the reaction will occur readily in the gas phase, where relaxation of the vibrationally excited molecules of **1** is slow. In the liquid phase where the internal excess energy of the molecules is dissipated more efficiently (via collisional deactivation), it is likely that most **1** will relax before isomerization to **1c**. It is worth noting that the calculated dipole moment of **SATS1** (3.27 D) is smaller than that of **SA1** (3.86 D). Therefore, it seems reasonable to conclude that the **1** → **1c** isomerization will not be favored in polar solvents, due to less effective dielectric stabilization of the less polar transition state.

3. Internal Rotation about the CO Bond. Previous ab initio calculations have assumed that the formal *syn/anti* isomerization of singlet **1** via twisting of the CH_2 group about the CO bond axis takes place via a perpendicular transition structure of C_s symmetry in which the plane of the carbon atom (sp^2 hybridization) has been rotated 90° with respect to the planar equilibrium geometry of singlet **1**. In contrast, we have

found that the rotation of the HCH plane about the CO bond leads to a substantial pyramidalization at the carbon atom. As a consequence, depending on the orientation of the HCH plane with respect to the OO bond, there are two possible conformations of the transition state. In fact, we have located the **SATS2** and **SATS3** transition structures of C_s symmetry on the conformational PES of singlet **1**. Both transition structures correspond to the same electronic state (^{1}A″) and have nearly identical geometrical parameters except that in **SATS3** the CH_2 group is directed toward the OO bond, while in **SATS2** it is directed outward. At all levels of theory **SATS3** is predicted to be somewhat less energetic than **SATS2**. As anticipated from the significant double bond character predicted for the CO bond of **1**, the rotation of the CH_2 group about the CO bond involves a high energy barrier. This is calculated to be at least 25.7 kcal/mol (via **SATS3**). Therefore, the formal *syn/anti* isomerization by rotation of the CH_2 group about the CO bond should be slow in the gas phase compared to other reactions of singlet **1**. Again it is worth noting that the calculated dipole moments of **SATS2** (2.41 D) and **SATS3** (2.23 D) are smaller than that of **SA1** (3.86 D). Consequently, it seems reasonable to conclude that the rotation of the CH_2 group about the CO bond will not be favored in polar solvents.

At this point it is noteworthy that the geometry of **SATS3** is very similar to that calculated for **TA2**. This result can be rationalized by noting that these structures belong to electronic states of the same symmetry (A″) and that the corresponding MRDCI wave functions have the same dominant electronic configuration (... $10a'^1\ 3a''^1$). The different spatial localization of the singly occupied orbitals 10a′ and 3a″ noted above suggests that the exchange integral, causing most of the ^{1}A″−^{3}A″ energy splitting, should be small. In fact, from the MRDCI+Q/basis A energies (Table 1 of the supporting information), **SATS3** is calculated to lie only 1.6 kcal/mol *above* **TA2**. We will discuss the implications of these features in a following section.

4. Inversion at the Central Oxygen Atom. Earlier theoretical studies have reported a COO linear C_{2v} structure to be the transition state for the formal *syn/anti* isomerization of singlet **1** via opening of the OOC bond angle.[18,21a] It should be pointed out that the nature (minimum or saddle point) of this structure was not determined in those studies. We have located a stationary point on the singlet PES of **1** which corresponds to this C_{2v} structure. The OO and CO bond distances of its optimized geometry, labeled **SATS4**, are 0.140 Å longer and 0.089 Å shorter, respectively, than those in **SA1**. The harmonic vibrational analysis of **SATS4** showed two imaginary frequencies (5650*i* and 705*i* cm^{-1}), indicating that this structure is not a true transition state. Furthermore, at the MRDCI+Q/basis B level, **SATS4** is calculated to lie about 10 kcal/mol higher than the **SATS2** and **SATS3** transition structures. Consequently, the importance of the degenerate pathway leading to inversion about the CO bond axis is lessened, as compared with the formal *syn/anti* isomerization via twisting of the CH_2 group about the CO bond axis.

5. Oxygen Atom Loss. The dissociation of singlet **1** into the singlet ground state of formaldehyde ($^1A_1$) and the lowest singlet state of the oxygen atom (^{1}D) is predicted to be highly endothermic. The calculated dissociation energy of 32.1 kcal/mol (see Table 3) for this process is about 30% lower than the value of 47 kcal/mol estimated by Cremer *et al.*[21i] from CCSD(T)/TZ+2P calculations combined with thermochemical data. In clear contrast, the dissociation of the lowest triplet state of **1** (^{3}A″) into ground-state formaldehyde and the triplet ground state of the oxygen atom (^{3}P) is predicted to be exothermic by 40.7 kcal/mol.[52,53] GVB-CI calculations using a DZ basis set have predicted a dissociation energy of −53.8 kcal/mol.[16a] This result led Wadt and Goddard to conclude that the twisted ^{3}A″ state of **1** should fall apart, since a significant barrier for scission of the OO bond is not expected. Our calculations give strong support to this conjecture. Thus, we have found on the triplet PES of **1** a transition structure (**TATS3**) interconnecting **TA2** and the ground-state formaldehyde plus O (^{3}P), lying 3.7 kcal/mol above **TA2**. This transition structure closely resembles **TA2**, with the exception of the OO and CO bond distances which are 0.155 and 0.060 Å longer and shorter, respectively, and the pyramidalization at the carbon atom, which is negligible at the transition structure.

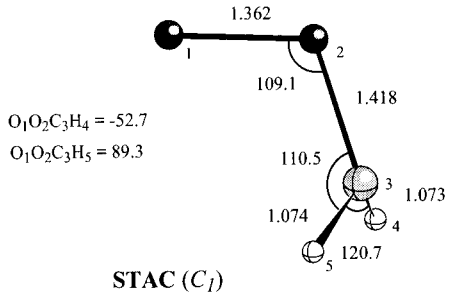

Figure 7. Selected geometrical parameters of the CASSCF/basis A calculated structure of a crossing point on the singlet−triplet crossing surface of formaldehyde carbonyl oxide. Distances are given in angstroms and angles in degrees.

As indicated in section I, the O-atom channel amounts to an estimated 1−5% of the total decomposition of the hot **1** generated in the gas-phase reaction of triplet methylene with O_2. On the basis that **1** generated in the less-energetic ethylene ozonolysis does not produce oxygen atoms at a detectable level, a substantial energy barrier is expected for the OO bond scission. Furthermore, since there is some evidence that the oxygen atoms are ejected in the triplet ground state, it is of interest to inquire about the mechanism of the oxygen atom loss from singlet **1**. In this regard we return to the point concerning the great similarity found between the geometries of **SATS3** and **TA2**, as well as the small energy difference (1.6 kcal/mol) between such structures. These features suggest a possible surface crossing between the lowest singlet and triplet states of **1** at some molecular geometries close to those of **SATS3** or **TA2**. In fact, an extensive CASSCF search using the dihedral angle (ϕ) between the OOC and HCH planes as a reaction coordinate led to the location of a structure ($\phi = 77.5°$), labeled **STAC** in Figure 7, where the singlet−triplet energy gap was calculated to be zero.[54] Consequently, this structure corresponds to a crossing point on the singlet−triplet crossing surface, or seam. In view of this, we propose that *the most reasonable pathway for the O-atom channel decomposition of hot singlet* ***1*** *involves rotation of the CH_2 group about the CO bond axis, followed by intersystem crossing (ISC) to the lowest triplet state and subsequent scission of the OO bond via the transition structure TATS3*.

It is worth mentioning that **STAC** is just one arbitrary point on the singlet−triplet crossing seam and not necessarily anywhere near the lowest energy crossing point. However, it is likely that this point lies energetically close to **STAC** since the overall triplet PES is nearly flat, the highest and lowest points

(52) At the MRDCI+Q/basis B level, the ^{1}D−^{3}P energy splitting in the oxygen atom is calculated (see footnote *a* in Table 3) to be 49.1 kcal/mol, compared with the experimental $^1D_2$−$^3P_2$ energy splitting of 45.4 kcal/mol.[53]

(53) Moore, C. E. *Atomic Energy Levels*; National Bureau of Standards Circular 467; U.S. Department of Commerce: Washington, DC, 1949.

(54) Calculated CASSCF(8,8)/basis A energies (hartrees): −188.67167 (singlet) and −188.67168 (triplet).

(i.e., **TA1** and **TATS3**) differing only by 2.4 kcal/mol at the CASSCF/basis A level. At this level of theory, **STAC** is calculated to lie 24.8 kcal/mol above **SA1**, that is, 2.2 kcal/mol above the transition structure for the cyclization of **1** to **1c**, **SATS1**. Thus, under conditions where the initially formed singlet **1** retains enough of the excess internal energy, the loss of oxygen atom should compete with isomerization to **1c**.

It is also useful to consider the relative efficiency with which ISC leads the ground-state singlet to the lowest triplet state. The probability of ISC induced by the spin−orbit coupling mechanism depends on the magnitude of the spin−orbit coupling matrix elements $\mathbf{H}_{IJ}^{SO}$ between the singlet and triplet wave functions near the singlet−triplet crossing seam.[55] The $\mathbf{H}_{IJ}^{SO}$ matrix elements were computed[56] (in a one-electron approximation using the effective nuclear charges of C (3.6) and O (5.6) optimized by Koseki et al.[57]) at **STAC**. The results were very small: 0.4 cm^{-1} for the parallel coupling (the $\mathbf{H}_{IJ}^{SO}$ matrix element connecting the singlet state and the $M_S = 0$ component of the triplet state) and 5 cm^{-1} for the perpendicular coupling (the $\mathbf{H}_{IJ}^{SO}$ matrix elements connecting the singlet state and the $M_S = -1$ and $+1$ components of the triplet state). Thus, while the ISC induced by the spin−orbit coupling mechanism is operative, it will not be efficient. Both the fact that singlet−triplet intersection is predicted to occur at very high energy and the low efficiency of the ISC (spin−orbit coupling) suggest that the O atom channel decomposition mode of singlet **1** is not easily accessible. This suggestion is in good agreement with the experimental observation that the O atom channel contributes to an estimated 1−5% of the total carbonyl oxide consumption.[14a]

B. Acetaldehyde Carbonyl Oxide. 1. Singlet and Triplet Equilibrium Structures. As far as we know, there are neither experimental data nor geometrical results from high-level ab initio calculations to judge the reliability of our structural predictions regarding the equilibrium structures of **2** and **2c**. In comparing the geometrical parameters of the OOC moiety of the structures optimized for the *syn* (**SB1**) and *anti* (**SB2**) stereoisomers of singlet **2** with those of **SA1**, it is found that the substitution of a hydrogen atom by a methyl group in the parent carbonyl oxide **1** causes a small elongation (about 0.03 Å) of the OO bond distance and a slight shortening (about 0.01 Å) of the CO bond distance. However, such a substitution increases the dipole moment by 0.45 (**SB1**) and 1.08 (**SB2**) D. On the other hand, it is interesting to note that in **SB1** a methyl hydrogen atom eclipses the adjacent methylene hydrogen atom, while in **SB2** these atoms are staggered. These results are in good agreement with early MP2 calculations with the 6-31G* basis set.[21a] Also in qualitative agreement with these calculations, we found the *syn* isomer to be 2.2 kcal/mol less energetic than the *anti* isomer. As regards the equilibrium structure calculated for **2c** (**SB3**), it is noteworthy that the plane defined by a CH bond of the methyl group and the CC bonds bisects the plane of the OCO ring. A comparison of geometrical parameters of **SB3** and **SA2** reveals that the substitution of a hydrogen atom by a methyl group in the parent dioxirane **1c** does not cause any significant change in the geometry of the three-membered ring. Furthermore, this substitution increases the dipole moment by only 0.18 D. The most remarkable geometrical feature of the equilibrium structure calculated for singlet hydroperoxyethylene (**SB4**) is the nearly planar *cis* conformation arrangement of the four heavy atoms. It is also worth mentioning that the calculated OO bond distance of 1.478 Å is somewhat longer than the experimental OO bond distance (1.452 Å) in hydrogen peroxide.

Regarding the lowest triplet state of **2**, the equilibrium structures **TB1**, **TB2**, and **TB3** can be envisaged as derived from those of the parent triplet **1** (**TA1** and **TA2**) by substituting a hydrogen atom by a methyl group. Since the two hydrogen atoms in **TA1** are not equivalent, such a substitution leads to the different conformations **TB1** and **TB2**, the latter being predicted to be 3.0 kcal/mol more energetic than the former. **TB3**, the structure formally derived from the lowest equilibrium structure of triplet **1**, **TA2**, by the aforementioned substitution, is energetically nearly degenerate with **TB1**. The common feature of the equilibrium structures **TB1**, **TB2**, and **TB3** is that the OO bond distances and the OOC bond angles are nearly identical to those of the corresponding unsubstituted equilibrium structures (**TA1** and **TA2**), while the CO bond distances are slightly longer (about 0.01 Å). Analogously, the rotational transition structures **TBTS1**, **TBTS2**, and **TBTS3** connecting the **TB1**, **TB2**, and **TB3** minima can be formally derived from the rotational transition structures **TATS1** and **TATS2** of triplet **1** by substituting a hydrogen atom by a methyl group. Thus, the OO bond distances and the OOC bond angles of **TBTS1**, **TBTS2**, and **TBTS3** are nearly identical to those of **TATS1** and **TATS2**, while the CO bond distances are somewhat longer. Therefore, it can be concluded that the substitution of a hydrogen atom by a methyl group in the lowest triplet state of **1** does not cause any significant change in the geometry of the COO moiety of the structures calculated for the stationary points on its PES.

2. *Syn/Anti* Interconversion. The *syn* (**SB1**) and *anti* (**SB2**) equilibrium structures of **2** are connected by the transition structures **SBTS3** and **SBTS4**, which can be formally derived from the transition structures **SATS3** and **SATS2**, respectively, of the parent carbonyl oxide **1** by substituting a hydrogen atom by a methyl group. **SBTS3** is calculated to be 2.5 kcal/mol less energetic than **SBTS4**. As anticipated from the results found for the rotation of the CH_2 group about the CO bond in singlet **1**, the conversion of the *syn* isomer of **2** into the *anti* isomer involves an energy barrier of at least 30.5 kcal/mol (via **SBTS4**). Analogously, the conversion of the *anti* isomer into the *syn* isomer involves an energy barrier of at least 28.3 kcal/mol. Consequently, the *syn/anti* isomerization might be slow in the gas phase compared to other reactions of singlet **2**. Furthermore, it is worth noting that the calculated dipole moments of **SBTS3** (2.40 D) and **SBTS4** (2.61 D) are smaller than those of both **SB1** (4.31 D) and **SB2** (4.94 D). Consequently, it is likely that the interconversion of the *syn* and *anti* isomers of **2** will not be favored either in polar solvents. It is reasonable, therefore, to expect different reactivities for the *syn* and *anti* stereoisomers of **2**.

As found for **1**, the **SBTS3** and **SBTS4** structure on the singlet PES of **2** are very similar to the **TB3** and **TBTS1** structures located on the PES of the lowest triplet state of **2**. These results again can be rationalized in terms of the dominant electronic configuration of the MRDCI wave function of these structures, which turns out to be the same, and the fact that the singly occupied orbitals of such a configuration are localized on different atoms. The energy separation between the open shell singlet and triplet states arising from this configuration is expected to be small. In fact, from the MRDCI+Q/basis A energies (Table 2 of the supporting information), **SBTS3** is calculated to lie 4.4 kcal/mol above **TB3**, and **SBTS4** 1.7 kcal/mol below **TBTS1**.

(55) Yarkony, D. R. *J. Am. Chem. Soc.* **1992**, *114*, 5406.

(56) By using the one-electron terms of the Breit−Pauli Hamiltonian,[57] at the CAS-CI level with the A basis set employing two sets of orbitals. The core orbitals obtained from the CASSCF(8,8) calculation of the triplet state were used for the singlet state (the frozen core approximation),[58] and the active orbitals of the singlet state were reoptimized in a separate CASSCF(8,8) calculation. All calculations were accomplished using the GAMESS code.

(57) Koseki, S.; Schmidt, M. W.; Gordon, M. S. *J. Phys. Chem.* **1992**, *96*, 10768.

(58) Lengsfield, B. H., III; Jafri, J. A.; Philips, D. H. *J. Chem. Phys.* **1981**, *74*, 6489.

3. Cyclization to Methyldioxirane. As a consequence of the predicted configurational stability of the *syn* and *anti* stereoisomers of **2**, there are two different transition structures for its isomerization to **2c**. One (**SBTS1**) connects the equilibrium structure of the *syn* isomer (**SB1**) with that of **2c** (**SB3**), while the other (**SBTS2**) connects the equilibrium structure of the *anti* isomer (**SB2**) with **SB3**. A comparison of these transition structures with that calculated for the cyclization of the parent carbonyl oxide **1** (**SATS1**) indicates that the methyl substituent causes a small elongation (about 0.04 Å) of the OO bond distance and a slight shortening (about 0.02 Å) of the CO bond distance. These geometrical changes are roughly the same noted above for the equilibrium structures **SB1** and **SB2**. In contrast to the small geometrical changes caused on both the reactant and transition state of the **1** → **1c** cyclization, the substitution of a hydrogen atom by a methyl group in **1** has a significant effect on the corresponding energy barrier. Thus, the energy barriers for the cyclization of the *syn* and *anti* isomers of **2** are calculated to be 28.4 and 20.6 kcal/mol, respectively, while that of **1** is 24.0 kcal/mol. On the other hand, the exothermicity of 28.2 kcal/mol calculated for the cyclization of the *syn* isomer of **2** is only 0.3 kcal/mol lower than that calculated for the cyclization of **1**. Assuming the same preexponential factor of the thermal Arrhenius expression of the rate constant for the **1** → **1c** and **2** → **2c** isomerizations, *it can be concluded that in the gas phase the cyclization of the anti isomer of **2** into **2c** should be faster than that of the parent carbonyl oxide **1** into **1c**, while the cyclization of the syn isomer should be slower than the latter*.

Regarding the cyclization in the liquid phase, it is worth noting that the calculated dipole moment of **SB1** (4.31 D) is larger than that of **SBTS1** (3.96 D), and that of **SB2** (4.94 D) is also larger than the dipole moment of **SBTS2** (4.42 D). Therefore, it is plausible that the cyclization of either the *syn* or *anti* isomer of **2** into **2c** will not be favored in polar solvents.

4. Oxygen Atom Loss. The dissociation of singlet **2** into the singlet ground state of acetaldehyde (^{1}A) and O (^{1}D) is predicted to be a highly endothermic process (see Table 3). Thus, for the *syn* and *anti* isomers of **2** the dissociation energy is calculated to be 31.8 and 29.6 kcal/mol, respectively. On the other hand, the dissociation of the lowest triplet state of **2** (i.e., **TB1**) into the ground state of acetaldehyde and O (^{3}P) is predicted to be exothermic by 47.0 kcal/mol. As in the case of the parent carbonyl oxide **1**, this suggests a low energy barrier in the lowest triplet state of **2** for scission of the OO bond. In fact, we have found a transition structure (**TBTS4**) interconnecting **TB3** and the ground-state acetaldehyde plus O (^{3}P) lying only 0.5 kcal/mol above **TB3**. This transition structure closely resembles **TB3**, with the exception of the OO and CO bond distances which are 0.151 and 0.063 Å longer and shorter, respectively, at the transition structure.

The greater similarity found between the geometries of **SBTS3** and **TB3**, as well as the small energy difference (4.4 kcal/mol) between such structures, again suggests a surface crossing between the lowest singlet and triplet states of **2** at some molecular geometries close to those of **SBTS3** or **TB3**. We have not attempted the location of any structure corresponding to a crossing point on the singlet−triplet crossing surface. However, as in the case of **1**, it is likely that the most reasonable pathway for the O-atom channel decomposition of hot singlet **2** involves the rotation of the $CHCH_3$ moiety about the CO bond axis, followed by ISC to the lowest triplet state and subsequent scission of the OO bond via the **TBTS4** transition structure. From the MRDCI+Q plus ZPVE correction energies (Table 2 of the supporting information), **TB3** is calculated to lie 28.9 and 26.7 kcal/mol above **SB1** and **SB2**, respectively. It can be concluded, therefore, that the O-atom channel decomposition mode of singlet **2** is not easily accessible. This conclusion is consistent with the results obtained in stopped-flow studies of gas-phase ozonation of *trans*-butene suggesting that the O-atom channel contributes on the order of $\leq$5% to the decomposition of **2**.[28b]

5. Tautomerization to Hydroperoxyethylene. The tautomerization of the *syn* isomer of singlet **2** to hydroperoxyethylene is predicted to be exothermic by 20.2 kcal/mol with an energy barrier of 21.2 kcal/mol. The transition structure calculated for this isomerization (**SBTS5**) shows a nearly planar five-membered ring where the migrating H atoms is linked to the terminal carbon and oxygen atoms through long bond distances (i.e., R(CH) = 1.382 Å, R(OH) = 1.322 Å). This indicates, no unexpectedly, that only the *syn* isomer of singlet **2** has the adequate spatial arrangement of the four heavy atoms to undergo tautomerization to hydroperoxyethylene. Since the conversion of the *anti* isomer into the *syn* isomer has an energy barrier of at least 28.3 kcal/mol (via **SBTS4**), the tautomerization of the *anti* isomer to hydroperoxyethylene should be slow in the gas phase compared to other reactions such as its cyclization to **2c**, which has a lower energy barrier of 20.6 kcal/mol. In contrast, the tautomerization of the *syn* isomer to hydroperoxyethylene, involving an energy barrier of 21.2 kcal/mol, should be faster than its isomerization to **2c**, which has an energy barrier of 28.4 kcal/mol. Therefore, if one assumes that the *syn* and *anti* isomers of singlet **2** are formed in comparable amounts in the gas-phase ozonation of *trans*-butene, one can make the prediction that *the fraction of **2** decomposed via tautomerization to hydroperoxyethylene should be on the same order as the fraction of **2** decomposed via cyclization to **2c***. This prediction is consistent with experimental results on the gas-phase ozonation of *trans*-butene suggesting that at least 10% of the total carbonyl oxide **2** formed decomposes via the hydroperoxide channel and also at least 10% of it decomposes via the isomerization to **2c** pathway.[28b] Furthermore, on the basis of the significantly lower energy barrier calculated for the hydroperoxide channel of the *syn* isomer of **2**, as compared to the energy barrier calculated for its isomerization to **2c**, it is reasonable to predict for methyl-substituted carbonyl oxides with a methyl group adjacent (*syn*) to the terminal oxygen that the tautomerization to the corresponding hydroperoxide should clearly dominate over the isomerization to the corresponding dioxirane. Once again this prediction agrees with experimental results on the gas-phase ozonation of tetramethylethylene suggesting that 80% of the acetone carbonyl oxide formed follows tautomerization to 2-hydroperoxypropylene, while isomerization to dimethyldioxirane is negligible.[28a]

V. Conclusions

Our theoretical investigation of the CH_2O_2 and $C_2H_4O_2$ singlet and triplet potential energy surfaces in the regions concerning the most relevant unimolecular reactions of formaldehyde and acetaldehyde carbonyl oxides reveals several important points.

(1) The *syn* stereoisomer of acetaldehyde carbonyl oxide is predicted to be 2.2 kcal/mol less energetic than its *anti* stereoisomer. The interconversional energy barriers of these stereoisomers are calculated to be at least 30.5 kcal/mol (*syn*) and 28.3 kcal/mol (*anti*). It is reasonable, therefore, to expect different reactivities for the *syn* and *anti* stereoisomers of acetaldehyde carbonyl oxide.

(2) The isomerization of formaldehyde carbonyl oxide to dioxirane is calculated to be exothermic by 28.5 kcal/mol with an energy barrier of 24.0 kcal/mol. The substitution of a hydrogen atom by a methyl group in this carbonyl oxide has a significant effect on the corresponding energy barrier, while such

a substitution has little effect on the energy of reaction. Thus, the energy barriers for the cyclization of the *syn* and *anti* stereoisomers of acetaldehyde carbonyl oxide into methyldioxirane are predicted to be 28.4 and 20.6 kcal/mol, respectively. The cyclization in the gas phase of the *anti* isomer of acetaldehyde carbonyl oxide should be faster than that of the parent carbonyl oxide, while the cyclization of the *syn* isomer should be slower than the latter.

(3) The dissociation of the singlet ground state of both formaldehyde and acetaldehyde carbonyl oxides into the singlet ground state of the corresponding carbonyl compound and the lowest singlet state of the oxygen atom (^{1}D) is predicted to be highly endothermic. In contrast, the dissociation of the lowest triplet state of both carbonyl oxides into the singlet ground state of the corresponding carbonyl compound and triple ground state of the oxygen atom (^{3}P) is predicted to be highly exothermic with a low energy barrier (i.e., 3.7 and 0.5 kcal/mol for formaldehyde and acetaldehyde carbonyl oxides, respectively). For the parent carbonyl oxide, a surface crossing between the lowest singlet and triplet states is found at twisted geometries of the singlet state close to that calculated for the equilibrium structure of the triplet state. Therefore, a reasonable pathway for the oxygen atom loss from hot singlet carbonyl oxides involves an internal rotation about the CO bond axis, followed by ISC to the lowest triplet state and subsequent scission of the OO bond. Since the surface crossing between the lowest singlet and triplet states is predicted to occur at very high energy, the oxygen atom loss from carbonyl oxides competes with the cyclization to the corresponding dioxirane. Moreover, the efficiency of the ISC (spin−orbit coupling) is predicted to be low, so the O-atom channel decomposition mode of singlet carbonyl oxides is not easily accessible.

(4) The tautomerization of the *syn* stereoisomer of acetaldehyde carbonyl oxide to hydroperoxyethylene is predicted to be exothermic by 20.2 kcal/mol with an energy barrier of 21.2 kcal/mol. Therefore, this isomerization competes favorably with the cyclization to methyldioxirane. In contrast, since the tautomerization of the *anti* stereoisomer requires a previous *anti* → *syn* conversion, which involves an energy barrier 7.7 kcal/mol higher than that calculated for its cyclization, the tautomerization of the *anti* stereoisomer of acetaldehyde carbonyl oxide cannot compete with its cyclization to methyldioxirane. For methyl-substituted carbonyl oxides with a methyl group adjacent (*syn*) to the terminal oxygen atom, it is predicted, in general, that the tautomerization to the corresponding hydroperoxide should clearly dominate over the isomerization to the corresponding dioxirane.

Acknowledgment. This research was supported by the Dirección General de Investigación Científica y Técnica (DGICYT Grants PB92-0796-C01 and PB92-0796-C02). Calculations described in this work were performed on two IBM RS6000 workstations at the Centre d'Insvestigació i Desenvolupament del CSIC, on the CONVEX C-3480 at the Centre Europeu de Paral·lelisme de Barcelona (CEPBA), and on the IBM 3090/600J at the Centre de Supercomputació de Catalunya (CESCA). The authors also wish to thank Professor Sigrid D. Peyerimhoff and Dr. Michael W. Schmidt for providing a copy of MRD-CI and GAMESS codes, respectively.

Supporting Information Available: Tables giving the Cartesian coordinates, total energies, zero-point vibrational energies, and dipole moments of all structures reported in this paper, the harmonic vibrational frequencies and infrared intensities of the equilibrium structures, and the vertical electronic excitation energies for the singlet ground state of **1** and **2** (25 pages). This material is contained in many libraries on microfiche, immediately follows this article in the microfilm version of the journal, can be ordered from the ACS, and can be downloaded from the Internet; see any current masthead page for ordering information and Internet access instructions.

JA953858A